Instability of Metastable Solid Solutions and Crystal to Glass Transition

Mo Li and William L. Johnson
W. M. Keck Laboratory, 138-78, California Institute of Technology, Pasadena, California 91125

(Received 27 July 1992)

Crystal to glass transitions are simulated using molecular dynamics for an fcc binary random solid solution with varying atomic size ratios and concentrations. The transition occurs at a critical supersaturated solute concentration with a sufficiently large solute-solvent atomic size difference. Close to the amorphization, the shear elastic moduli become dramatically softened, accompanied by a martensite-like structural change. Large strain fluctuations and small enthalpy and volume changes at the transition indicate that it is triggered by a mechanical instability reached in the metastable crystal.

PACS numbers: 61.43.Fs, 64.70.Pf, 65.50.+m, 82.20.Wt

Metastable metallic glasses are conventionally prepared by rapid quenching of melts at cooling rates from 10^4–10^7 K/s. In the last two decades, it has been found that glassy or amorphous phases can also form from crystalline solids [1]. Such crystal to glass transformations (CGT) occur when the crystal is driven far from equilibrium into a metastable state while subjected to certain kinetic constraints. The CGT has been observed during irradiation of solids with high-energy particles [2], hydrogen absorption by crystalline intermetallics [3], severe mechanical deformation of crystals [4], and solid-state interdiffusion reactions of elemental metals [5]. In addition to its technological interests, the CGT has been studied in relation to ordinary melting [1,6]. Further, it raises interesting questions in relation to the glass transition of undercooled liquids [7]. Although progress has been made recently [8], present understanding of the thermodynamics and microscopic mechanisms underlying this transformation is rather incomplete. As in the case of liquid to glass transitions, there are problems in defining a suitable order parameter for the transformation. It is difficult to characterize this transition thermodynamically since the system is typically not in equilibrium. The crystal is frequently driven to evolve along competing pathways. For example, chemical segregation and/or formation of more stable crystalline phases are frequently observed in experiments [1,9]. Furthermore, in real crystals, defects and imperfections, surfaces and interfaces, etc., may serve as preferred nucleation sites for new phases and thereby complicate experimental observations. Computer simulation provides an alternative method which eliminates some of the problems encountered in experiments. With this method, it is possible to study the atomic structure, thermodynamic, and dynamic properties of metastable systems at the CGT.

In the present work we ask the following questions: What thermodynamic stability limit does the metastable crystalline system reach when the CGT occurs and under what conditions? How is the CGT related to melting and liquid to glass transitions if both liquids and crystals are made metastable? In this Letter, we present results from molecular dynamics (MD) simulations of metastable binary solid solutions to address the first question. This is one of a series of theoretical and experimental attempts to understand solid-state amorphization and melting [1,10].

Binary solid solutions are chosen because they are simple to characterize and have been extensively studied both theoretically and experimentally. The results from modeling thermodynamic properties of liquid and solid mixtures [11], rationalizing solute solubilities [12], and predicting glass-forming tendencies by rapid quenching [13] all provide useful background for the present work. The instability determining the limit of the equilibrium miscibility of the solid solution is the chemical instability. An equilibrium two-phase separation would occur if the solute concentration exceeds the limit. The equilibrium miscibility can be obtained from Gibbs free energies of the equilibrium terminal solid solutions. However, extensive computations are required to obtain them. By using the results of the hard-sphere binary mixture [12], we estimated the equilibrium miscibility of the solid solution, which has roughly the same atomic size ratio between solute and solvent atoms with Lennard-Jones interactions, to be less than 5 at.%. The actual solute concentrations obtained in our calculations are far greater. The metastable supersaturated solid solutions are obtained by restricting long-range diffusion and formation of clusters and short-range ordering. This is achieved by simply imposing certain constraints in simulations, that is, keeping the system at low temperature, using a finite sample with a periodic boundary condition and assuming the same Lennard-Jones (LJ) potential depth between all the solvent and solute atoms. Moreover, thermodynamic properties of such homogeneous metastable solid solutions are well defined, because the relaxation time of the metastable system is much greater than the simulation time.

To obtain desired structural variations and elastic properties at the CGT, a modified [14] rather than the original Parrinello-Rahman molecular dynamics (PRMD) [15] is used. This is because the original PRMD has been found to produce artificial structural distortions and free rotations of the MD cells as a whole, and thus results in incorrect lattice parameters and slow convergence or nonconvergence of calculated elastic constants and other thermodynamic properties. These nonphysical results become more pronounced and thus deleterious in simulations of systems with initial configurations far from equilibrium. In the present case, the lattice parameters of the solid solutions are unknown, so their initial configurations at each solute composition have to be assigned by assuming that the atoms are situated at the bottom of their potential wells and are completely randomly distributed on an initial lattice. Although it is a reasonable approximation, the method becomes inadequate for original PRMD close to the CGT, where large lattice relaxation and atom rearrangement occur. With the modified PRMD in which the MD cell kinetic energy is modified to take into account its invariance with respect to translational symmetry, stable MD cells free of artificial distortion and rotation can be obtained in spite of the choices of initial lattice structures. The calculations are made using 500 atoms for a constant pressure and temperature, which are set to 0.0 and 0.3 (in reduced LJ units), respectively. The corresponding glass transition temperature in the LJ liquids $T_g \approx 0.40$. The volume and the shape of the MD cell is allowed to fluctuate and thus a constant (*NPT*) ensemble is achieved in the MD simulations.

LJ potentials are used for the interactions between solute and solvent atoms,

$$\phi_{\alpha\beta}(r_{ij})=4\epsilon_{\alpha\beta}\left[\left(\frac{\sigma_{\alpha\beta}}{r_{ij}}\right)^{12}-\left(\frac{\sigma_{\alpha\beta}}{r_{ij}}\right)^{6}\right], \qquad (1)$$

where α,β denote the two types of atoms, *A* and *B*. It is assumed that $\epsilon_{AA}=\epsilon_{AB}=\epsilon_{BB}=\epsilon$. The other LJ potential parameters, σ_{AA} and σ_{BB}, are proportional to the sizes of atoms. For simplicity we assume $\sigma_{AB}=\frac{1}{2}(\sigma_{AA}+\sigma_{BB})$ and $\sigma_{AA}=\sigma$. The only intrinsic "defects" which disrupt the crystalline states are the atomic size differences between solute and solvent atoms. Therefore, only two parameters are needed to characterize the system at a given pressure and temperature. They are the atomic size ratio $\alpha=R_{BB}/R_{AA}=\sigma_{BB}/\sigma_{AA}$, where R_{AA} and R_{BB} are the radii of *A* and *B* atoms, and the concentration of the solute $x_B=N_B/N$, where N_B and N are the number of *B* atoms and the total number of atoms, respectively.

Metastable solid solutions at the given *P* and *T* are simulated for different α and x_B, as indicated on the phase diagram in Fig. 1. For each solid solution with a given atomic size ratio and solute concentration, an fcc crystalline structure with the small solute atoms randomly distributed on the lattice sites is taken as the initial configuration. The equilibrium configuration is reached after annealing. Average thermodynamic properties such as enthalpies and elastic constants are obtained in the equilibrated samples following the annealing.

Figure 1 shows that the CGT occurs only when the atomic size difference is sufficiently large. For $\alpha=0.85$ the solid solutions remain crystalline for the entire solute concentrations. At large solute concentration, a martensite-like structural distortion, where the fcc lattice transforms to a fct lattice, is observed. In this Letter, we will present results of the CGT obtained for a smaller atomic size ratio than the critical one, α_c, which is close to 0.83 in the LJ solid solutions at the given *P* and *T*.

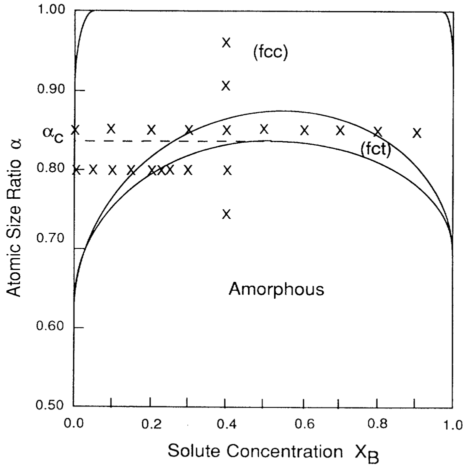

FIG. 1. Schematic metastable phase diagram in parameter space (α, x_B) at constant *T* and *P* for the LJ binary solid solution. × marks the phases calculated from MD. The areas at the two upper corners are the equilibrium terminal LJ solid solutions.

Figure 2 shows the total and partial pair correlation functions (PCF) obtained after annealing as the solute concentration increases at fixed atomic size ratio $\alpha=0.80$, or 20% size difference. Below $x_B=0.20$, the PCF clearly shows a fcc structure. The partial PCF of *AA*, *AB*, and *BB* atoms and their first and second nearest-neighbor coordination numbers suggest no local clustering or short-range chemical ordering. The peaks in the PCF are broadened with increasing solute concentration, but the crystallinity is still retained, indicating the crystals are progressively disordered. Beyond $x_B=0.20$, the PCF shows a qualitatively different form which resembles that commonly found in liquids and amorphous metals. The split second peaks in the PCF which are usually used as a signature for the formation of glassy structures are readily seen, especially in the partial PCF.

Figures 3(a) and 3(b) show the tetragonal shear modulus $C'=(C_{11}-C_{12})/2$ and rhombohedral shear modulus C_{44} versus composition at fixed atomic size ratio ($\alpha=0.80<\alpha_c$). Both shear moduli decrease with increasing solute concentration. The magnitude of the shear moduli softening as the CGT is approached is remarkable. At $x_B=0.2$, just prior to amorphization, the tetragonal shear modulus drops nearly 70% from its initial value at $x_B=0.0$ and shows a deep cusp. The rhombohedral shear modulus, however, is less sensitive to solute concentration. It decreases slowly at low concentrations and much more rapidly close to or at the critical

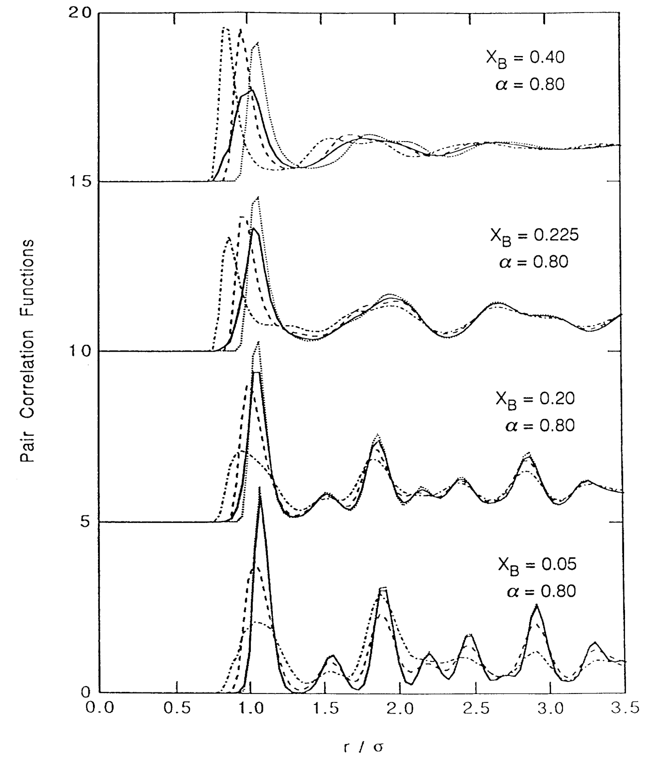

FIG. 2. Partial and total pair correlation functions of fcc crystalline solid solutions at different solute concentrations. The solid line is for ρ_{total}; the dashed line is for ρ_{AB}; the dotted line is for ρ_{AA}; and the dot-dashed line is for ρ_{BB}.

concentration x_c. The crystalline state persists even into the region where C_{44} shows relatively large softening. The two shear moduli approach the same isotropic value ($\approx 25.0 N k_B T/V$) when the amorphous phase forms.

Figure 3(c) shows the molar enthalpy and molar volume versus composition. The changes of both the molar volume and molar enthalpy are extremely small ($< 1\%$) across the CGT boundary. However, their slopes are different on both sides of the transition. The molar enthalpy on the amorphous side also shows a very slow increase with increasing composition.

The tremendous softening of the shear elastic responses indicates that the metastable crystal loses its shear rigidity against large shear strain fluctuations. When this happens, it is expected that a structural distortion along the shear-softened direction would occur. Indeed, a martensite-like structural distortion close to the critical composition x_c has been observed where the fcc structure transforms to a fct structure. Additional skewing of the MD cell occurs in the amorphous phase region, and upon further increasing x, it becomes cubic again. We did not obtain near-zero shear elastic constants near x_c; this may be due to large structural fluctuations and the finite sample size used. Nevertheless, our results do show extremely large shear strain fluctuations and very small enthalpy and volume change at the CGT and thus suggest that the

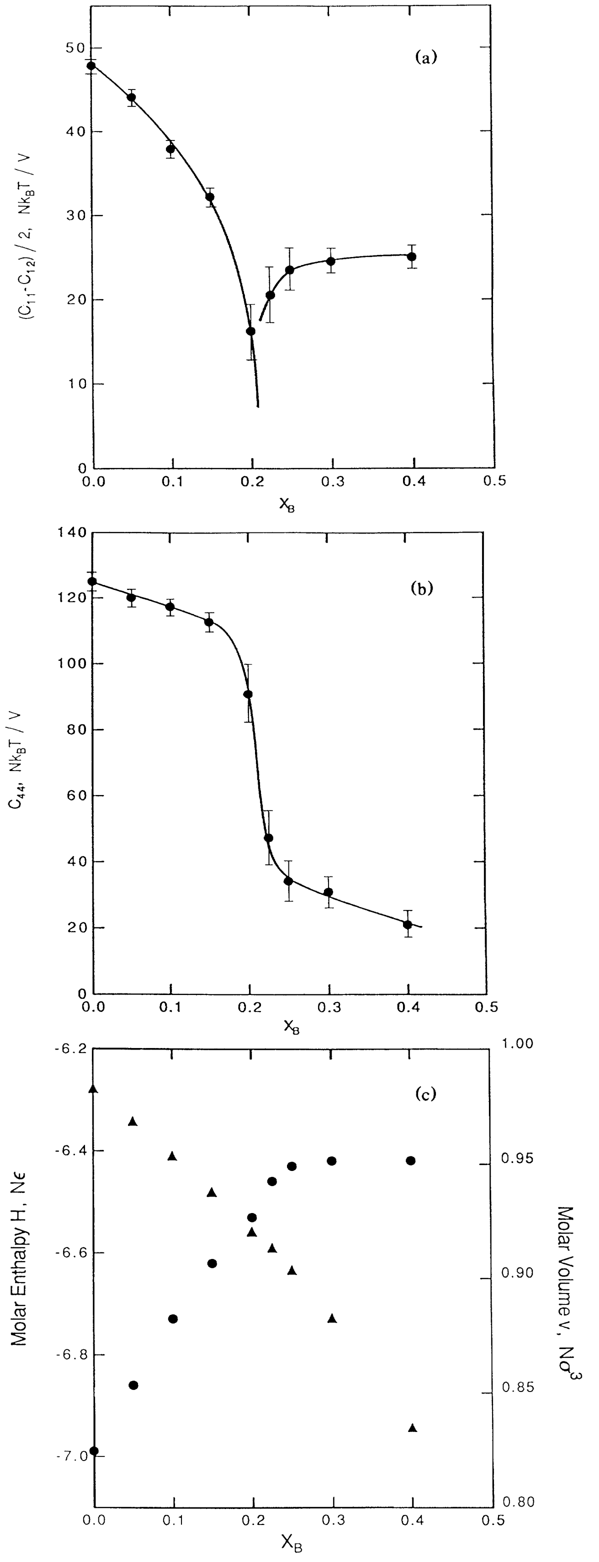

FIG. 3. (a) Isothermal tetragonal shear modulus; (b) isothermal rhombohedral shear modulus; (c) the molar enthalpy (dots) and volume (triangles) vs compositions at the fixed atomic size ratio. The solid lines are drawn to guide the eyes.

CGT is likely continuous or weakly first order (even though it may not be reversible). The metastable crystalline solid solution seems to have reached a mechanical instability characterized by a vanishing elastic shear stiffness C', or a diverging elastic compliance $1/C'$ at x_c. In the past, thermodynamic instabilities characterized by vanishing elastic moduli have been referred to as mechanical instabilities [1,6,16]. Although phase transitions triggered by this type of instability are not as often observed as those due to thermal or chemical instabilities, thermal martensite transitions and displacive structural phase transitions characterized by one type of vanishing shear elastic modulus or another [17] are among those few frequently encountered. Elastic shear modulus softening has been observed by Brillouin scattering [18] from the intermetallic compound Zr_3Al during irradiation. The average shear wave velocity decreases continuously in the progressively disordered crystal under irradiation. When the CGT occurs, it drops to nearly 40% of its value in the ordered crystal. Since averaged sound velocity is measured, the particular shear instability responsible for the CGT has not been identified.

These results lead us to speculate that the CGT is caused by frustration of local *shear* deformations within the crystal. The large elastic anisotropy C_{44}/C' close to the CGT indicates that the transition involves changes of crystalline orientations mainly through *tetragonal shearing* and gradual reduction of the orientation correlations caused by introduction of quenched-in atomic defects. In the metastable random binary solid solution, the atomic size mismatch creates local random stress fields which locally favor a particular variant (three variants in the case of tetragonal distortion and four in the case of rhombohedral distortion) in much the same manner that a random field locally favors a specific spin orientation in local domains of random field spin systems [19]. In the case of the spin system, above a critical strength, the random field leads to the formation of a spin glass. When the random shear stress field created by atomic size mismatch is not strong enough, the long-ranged crystalline orientational and translational order are still present. The tetragonal shear softening in the lattice leads to martensite-like structural distortion to a fct structure with long-range tetragonal symmetry. Experiments on real supersaturated metastable solid solutions have confirmed this finding. It was found that prior to the CGT, tetragonal structural distortions are observed in the form of distorted metastable crystalline phases with local tweeded structures [9,20]. Further increase of solute concentration towards x_c will lead to destruction of the orientational order and translational order as well [21]. In the present case, the effects of local random shear stress fields frustrate the local shear deformations of the atoms and result in a structural glass. Further results on this subject will be presented elsewhere.

Support for this work was provided by a grant from the DOE under Contract No. DE-FG03-86ER45242 and by Materials & Molecular Simulation Center at Caltech.

---

[1] W. L. Johnson, Prog. Mater. Sci. **30**, 81 (1986).

[2] *Phase Transformations During Irradiation,* edited by F. V. Nolfi (Applied Science, Englewood, NJ, 1983).

[3] X. L. Yeh *et al.*, Appl. Phys. Lett. **42**, 242 (1983); U. I. Chung *et al.*, Philos. Mag. B **63**, 1119 (1991).

[4] C. C. Koch *et al.*, Appl. Phys. Lett. **43**, 1017 (1983); R. B. Schwarz *et al.*, J. Non-Cryst. Solids **76**, 281 (1985); Q. Williams and R. Jeanloz, Science **239**, 902 (1988).

[5] R. B. Schwarz and W. L. Johnson, Phys. Rev. Lett. **51**, 415 (1983); S. R. Herd *et al.*, Appl. Phys. Lett. **42**, 597 (1983).

[6] D. Wolf *et al.*, J. Mater. Res. **5**, 286 (1990).

[7] J. P. Sethna *et al.*, Phys. Rev. B **44**, 4945 (1991).

[8] Y. Limoge and A. Barbu, Phys. Rev. B **30**, 2212 (1984); C. Massobrio, V. Pontkis, and G. Martin, Phys. Rev. Lett. **62**, 1142 (1989); H. Hsieh and S. Yip, Phys. Rev. Lett. **59**, 2760 (1987); M. J. Sabochick and N. Q. Lam, Phys. Rev. B **43**, 5243 (1991).

[9] C. Krill III, Ph.D thesis, California Institute of Technology, 1992.

[10] W. L. Johnson and M. Li, J. Non-Cryst. Solids (to be published).

[11] W. G. T. Kranendonk and D. Frenkel, J. Phys. Condens. Matter. **1**, 7735 (1989); A. R. Denton and N. W. Ashcroft, Phys. Rev. B **43**, 3161 (1991); and references therein.

[12] W. Hume-Rothery and B. R. Raynor, Proc. R. Soc. London A **174**, 471 (1954).

[13] T. Egami and Y. Waseda, J. Non-Cryst. Solids **64**, 113 (1984).

[14] M. Li and W. L. Johnson, Phys. Rev. B **46**, 5237 (1992); M. Li, W. L. Johnson, and W. A. Goddard III, in MRS Symposia Proceedings No. 291 (Materials Research Society, Pittsburgh, 1992).

[15] M. Parrinello and A. Rahman, Phys. Rev. Lett. **45**, 1196 (1980).

[16] M. Born, J. Chem. Phys. **7**, 591 (1939).

[17] R. N. Bhatt and W. L. McMillan, Phys. Rev. B **14**, 1007 (1976); G. R. Barsch and J. A. Krumhansl, Metall. Trans. A **19**, 761 (1988); B. Lüthi and W. Rehwald, in *Structural Phase Transitions I,* edited by K. A. Müller and H. Thomas (Springer-Verlag, Berlin, 1981), pp. 131–184.

[18] P. R. Okamoto *et al.*, J. Less-Common Met. **140**, 231 (1988).

[19] K. Binder and A. P. Young, Rev. Mod. Phys. **58**, 801 (1986).

[20] A. Peker and W. L. Johnson (unpublished).

[21] P. J. Steinhardt, D. R. Nelson, and M. Ronchetti, Phys. Rev. B **28**, 784 (1983).